Chemical Engineering Journal 425 (2021) 130489

Contents lists available at ScienceDirect

Chemical Engineering Journal

journal homepage: www.elsevier.com/locate/cej

The degradation mechanisms of *Rhodopseudomonas palustris* toward hexabromocyclododecane by time-course transcriptome analysis

Yi-Jie Li [a,1], Reuben Wang [b,1], Chung-Yen Lin [c], Shu-Hwa Chen [f], Chia-Hsien Chuang [c], Tzu-Ho Chou [a], Chi-Fang Ko [a], Pei-Hsin Chou [d], Chi-Te Liu [e], Yang-hsin Shih [a,*]

[a] Department of Agricultural Chemistry, National Taiwan University, No. 1, Sec. 4, Roosevelt Rd., Taipei, Taiwan
[b] Institute of Food Safety and Health, National Taiwan University, No. 1, Sec. 4, Roosevelt Rd., Taipei, Taiwan
[c] Institute of Information Science, Academia Sinica, No. 128 Academia Rd. Sec. 2, Taipei, Taiwan
[d] Department of Environmental Engineering, National Cheng Kung University, Tainan, Taiwan
[e] Institute of Biotechnology, National Taiwan University, No. 81, Chang-Xing St., Taipei, Taiwan
[f] TMU Research Center of Cancer Translational Medicine, Taipei Medical University, No. 250 Wu-Hsing St., Taipei, Taiwan

ARTICLE INFO

Keywords:
Rhodopseudomonas palustris
Hexabromocyclododecane
Transcriptome
Biodegradation
Metabolic pathway

ABSTRACT

Hexabromocyclododecane (HBCD) is one of the most frequently used brominated flame retardants (BFRs). However, the HBCD degradation method's development has become vital because it readily bioaccumulates and is persistent in the environment. A previous study showed *Rhodopseudomonas palustris* degrades HBCD through several possible metabolic pathways based on transcriptomic analysis of compared samples. This study introduces multiple time-course transcriptomic analysis approaches to identify the specific HBCD metabolic pathway in *R. palustris* inbubated at different temperatures. The transcriptome profiles revealed that the addition of HBCD triggered 126 transcripts in cells at 25°C and 35°C. Further KEGG analysis showed several HBCD induced metabolic pathways, including ABC transporter, butanoate metabolism, dephosphorylation, lipid glycosylation pathways, etc. The principal component analysis further provides evidence of genes directly affected by HBCD. The increased expression level of transcriptional regulator LysR, two-component system regulators, HBCD degradation enzymes, including haloacid dehalogenases, glutathione-S-transferase, cytochrome p450, hydrolases, and dioxygenases in *R. palustris* were confirmed by qRT-PCR analysis. Combining the transcriptomic profiles and gene expression level analysis, we proposed the HBCD metabolic pathway in *R. palustris*. Briefly, HBCD signal transferred from cell membrane to transcriptional regulator LysR, then further to downstream degradation working enzymes. Overall, our results highlight the value of systematic transcriptomic approaches to discover and elucidate the intrinsic microbial metabolisms for HBCD degradation in *R. palustris*. The results of this study provide a novel perspective on the degradation of persistent organic pollutants (POPs) such as HBCD using a bio-omics approach.

1. Introduction

Hexabromocyclododecane (HBCD) is one of the most frequently used brominated flame retardants (BFRs) alongside polybrominated diphenyl ethers (PBDEs) and tetrabromobisphenol A [1-3]. Since HBCD was first manufactured in the 1960s, its production capacity had reached more than 20,000 tonnes per year in the 2000s [4]. Because of the extensive use of HBCD as an additive flame retardant in textile and electronic products, and the fact that it had been declared as one of the persistent organic pollutants (POPs) by Stockholm Convention, and had been detected in a diverse range of environments, including water bodies, sediments, and poultries [2,5-8], it is vital to address the accumulation and the toxicity of HBCD in the environments.

Numerous environmental remediation measures for HBCD have been studied, ranging from physical or chemical approaches to more eco-friendly bioremediation methods. HBCD was eliminated in the UV/TiO_2/potassium persulfate homo/heterogeneous photocatalysis system [9]. Nanoscale zero-valent iron aggregates were also shown to remove HBCD through the debromination process rapidly in an aqueous solution [10]. Despite the high HBCD removal ratio of physiochemical

* Corresponding author at: Department of Agricultural Chemistry, National Taiwan University, No. 1, Sec. 4, Roosevelt Rd., Taipei 10617, Taiwan (R.O.C.).
E-mail address: yhs@ntu.edu.tw (Y.-h. Shih).
[1] These authors contributed equally.

https://doi.org/10.1016/j.cej.2021.130489
Received 8 March 2021; Received in revised form 6 May 2021; Accepted 20 May 2021

remediation approaches of HBCD, they pose technical and economic challenges. Bioremediation has long been considered an efficient, eco-friendly, and cost-effective measure to address a wide range of environmental contaminations [3,11,12]. *Pseudomonas* sp. HB01 was reported to remove 80 % of HBCD treated within 5 days [13]. *Pseudomonas aeruginosa* HS9 could degrade 70 % of 1.7 mg/L HBCD in 14 days by two metabolic pathways. One by series of debromination followed by oxidation pathways; and second through simultaneous debromination with hydroxylation process [14].

Rhodopseudomonas palustris is a phototrophic purple non-sulfur bacterium (PNSB) with one of the most versatile metabolisms known in bacteria. *R. palustris* can use both organics and inorganics, and light as an energy source. It can also get energies from chemoautotrophic, chemoheterotrophic, photoautotrophic, and photoheterotrophic metabolisms [15-18]. The highly adaptive characteristics and the diversity to metabolize organic compounds, such as aromatic pollutants or plant-derived compounds of *R. palustris* makes it ideal for bioremediation application [15,17]. In the previous study, HBCD was degraded by *R. palustris* strain YSC3 with the optimal removal condition at 35 °C, pH 7, and aerobic culture [19]. Despite the HBCD metabolites pentabromocyclododecenes (PBCDEs) and pentabromocyclododecanols (PBCDOHs) were found during the biotransformation process, the full scheme of functional genes and enzyme mechanisms were still unclear [19,20].

The advancement of the high-throughput sequencing technique allowed us to investigate the biodegradation of emerging organic contaminants with a more profound perspective and obtain detailed genomic, transcriptomic, and proteomic metagenome-guilded bioinformation. With the new insights from -omics approaches and the web-based analyses of gene ontology (GO terms) and Kyoto Encyclopedia of Genes and Genomes (KEGG) database, we can now address the contaminants in a more precise, eco-friendly, and efficient way [20,21]. Previously, Wang et al. [20] had proposed the possible molecular responses of *R. palustris* to HBCD degradation. However, with limited and late - observation time points, many possible crucial functional enzymes for initiating the HBCD degradation process were overlooked. Therefore, this study aims to uncover the functional genes, metabolic pathways, and *R. palustris* HBCD biotransformation system by the time course transcriptomics study.

2. Material and methods

2.1. Chemicals

Technical HBCD ($C_{12}H_{18}Br_6$) mixture (95 % purity) was purchased from Sigma-Aldrich (USA) and was dissolved in dimethyl sulfoxide as a stock solution (50 mg/L). PNSB medium was used to cultivate the bacteria [18]. The composition of PNSB medium was as followed (per 1 L): KH_2PO_4, 1.0 g; NH_4Cl, 1.0 g; $MgSO_4{\cdot}7H_2O$, 0.2 g, $FeSO_4{\cdot}7H_2O$, 0.01 g; $CaCl_2$, 0.02 g, $MnCl_2{\cdot}4H_2O$, 0.002 g; $Na_2MoO_4{\cdot}2H_2O$, 0.001 g; yeast extract, 0.5 g; malate, 10.0 g; pH adjusted to 7.0 ± 0.05. The culture was incubated for 24 hr at 37 °C at 150 rpm to reach a optical density (OD) to the log phase of 0.4 OD_{600nm}/mL (~4×10^8CFU/mL).

2.2. R. Palustris batch experiments and chemical analysis

R. palustris YSC3 was used in this study was provided by Dr. Chi-Te Liu (Insitute of Biotechnology, National Taiwan University, Taiwan) [18-20]. The whole genome of *R. palustris* stain YSC3 was available in NCBI (CP019967.1) [18]. *R. palustris* was first activated and cultured with PNSB medium at 35 °C in the dark under aerobic conditions. Series of batch experiments were conducted with the time course of hours 0, 4, 12, 24, 48, and 72.

HBCD was extracted with 3-fold volume hexane to aqueous bacterial culture. The mixtures were vortexed under room temperature for 40 min followed by centrifuge at 5,000 × g for 5 min. The extraction process continued until the HBCD concentration of the extract was less than the detection limit. The analytical condition for HBCD was set as described previously [10,22]. In sum, the recovery rate for HBCD extraction reached 90 to 105 %. The concentration of HBCD was detected with a GC/micro-electron capture detector (Agilent, 6890 N) equipped with a DB-5HT column (15 m × 0.25 mm × 0.1 μm film, J&W). The analytical condition for HBCD was programmed as described previously [5,19,20]. In short, the injector temperature was 170 ℃ and the flow rate was 21.1 mL/min. The oven temperature was initially maintained at 150 °C for 0.5 min, and then increased to 300 °C at the rate of 50 ℃/min, and sustained for 2 min. The detector temperature was set to 300 °C.

2.3. RNA extraction and high throughput sequencing

The gene expression in response to HBCD treatment was analyzed with RNA-sequencing process. The RNA of *R. palustris* cell culture at 4 hr and 12 hr of incubation under 25 °C and 35 °C was extracted using Geneaid PrestoTM Mini RNA Bacteria Kit according to the manufacturer's protocol. The OD photometrically at 280 nm and 260 nm (NanoDrop ND-2000, Thermo-Fisher Scientific Inc., United States) were measured to assess the purity and quantity of the eluted total RNA. An OD $260_{nm}/280_{nm}$ ratio of greater than 1.8 was considered protein-free RNA. The cDNA library construction had followed the protocol of TruSeq RNA Library Prep Kit v2, and the resulting cDNA libraries were sequenced using Illumina HiSeq in single-end 101 nt format.

3. Functional annotation of *R. Palustris* genome and co-expression network analysis

R. palustris strain YSC3 assembled genome is generously provided by Dr. Chi-Te Liu also. The *R. palustris* YSC3 genome description had been discussed in the previous work [18,19]. In brief, the genome size is 5.3 Mb and has 4907 coding sequences (CDS) which can be translated into 4907 proteins. GO annotations were granted with detectable Pfam domains according to Pfam2GO. Furthermore, we mapped the protein-coding genes to the canonical pathway database KEGG pathway using KAAS (KEGG Automatic Annotation Server, http://www.genome.jp/tools/kaas/[23]).

RNA-seq raw files, FASTQ files, were processed by a docker, *docexpress_fastqc*, by us (available at https://hub.docker.com/r/lsbnb/docexpress_fastqc), which is supported by Linux container virtualization and Galaxy platform [24]. A complete workflow for computing the transcriptomic profile in each sample was deployed on this platform (Fig. S1). In short, each sample was preprocessed by Trim Galore (http://www.bioinformatics.babraham.ac.uk/projects/trim_galore/) [25] to control read quality by trimming adapter strings and low quality bases (Table S1). After quality control steps, reads were aligned to the *R. palustris* genome by HISAT2 [26], which is a fast and sensitive spliced alignment program. Then we used StringTie [27] to count read alignments to the presumed transcriptome. The output is the *R. palustris* transcriptional profiles in fragments per kilobase per million (FPKM) value [28]. Lastly, we load the transcriptional profiles into our developed web-based analysis platform, MOLAS (http://molas.iis.sinica.edu.tw, unpublished), for downstream analysis.

The *R. palustris* co-expression networks were constructed by the weighted gene co-expression network (package "WGCNA") [29,30] in R. Transcript expression profiles were used to build networks, and the trait "HBCD_Time" was used to create the plot of the module-trait relationship. For the intramodular analysis, the gene significance (GS) and module membership (MM) were defined as the absolute correlation value of transcript expression pattern to each trait or each module eigengene, respectively.

3.1. Analysis of differentially expressed genes (DEGs)

In order to identify the DEGs in each HBCD-treated group, the gene

expression profiles of each sample were first loaded into the genome analysis platform built-in MOLAS. The threshold of a gene to be considered as a DEG was set at the absolute value of log2-fold ($|\log_2 FPKM| \geq 2$) with p-value < 0.05. Therefore, we then had four DEG sets, including two of the 4 and 12-hour of HBCD treatment groups at 25 °C and the 4 and 12-hour of HBCD treatments at 35°C. As mentioned above, only genes with $\log_2$ FPKM$\geq$2 and $\log_2$ FPKM$\leq$2 were considered to be the up-regulated and downregulated genes, respectively. Besides, the DEGs with ($|FPKM| \geq 5$) of the 12-hours-HBCD-treatment group at 35 °C were randomly chosen for the principal component analysis (PCA) analysis (Table S2). This enables one to visually assess the similarities and differences between sample groups of the gene expression data.

The heatmap and hierarchical clustering analysis were implemented in R package "ComplexHeatmap" [31]. To explain the difference in gene expression between different treatments, we used z-scores of the raw value for the heatmap construction. Raw transcript values above the mean have positive z-scores and *vice versa*. The hierarchical clustering analysis of samples and transcripts was constructed by calculating the Euclidean distance and Spearman's rank correlation, respectively. Then objects were clustered by the average linkage, representing the distance between clusters was considered as the average distance from any member of one cluster to any member of the other cluster.

3.2. Quantitative real-time polymerase chain reaction

First-strand cDNA was synthesized from the extracted RNA (4 μg) by reverse transcription (RT) with SuperScript® IV First-Strand Synthesis System (Invitrogen™, Thermo-Fisher Scientific Inc., United States) and the random primers (for bacteria). The synthesized cDNA was stored at −20 °C. The primer design for qRT-PCR was conducted with NCBI PrimerBlast [32,33]. Primers with no additional terminal or other modifications were synthesized by Mission Biotech (Taipei, Taiwan). The qRT-PCR was carried out with the LightCycler 480 system (Roche, Germany) and SYBR Green mix (KAPA Biosystems, United States). All primer sequences are listed in Table. S1. Gene *clpX* was used as an internal standard [34,35]. Results are expressed as mean ± SD. The data were processed with LightCycler 480 software (Version 1.5). All tests were performed with three independent biological replicates. Statistical evaluations were performed using Student's *t*-test using GraphPad Prism version 5 (GraphPad Software, San Diego, CA, USA). A value of $p < 0.05$ was considered as statistically significant.

3.3. Genotoxicity test

The *Bacillus subtilis* Rec-assay was conducted to assess the possible genotoxicity of HBCD to *R. palustris*. Briefly, the survival rates of recombinant proficient strain (Rec^+) and recombinant deficient strain (Rec^-) were compared to evaluate the potential genotoxic effects of HBCD. 4-Nitroquinoline 1-oxide (4-NQO) was considered a positive control. The genotoxicity was calculated as R_{50}, the ratio of median inhibitory concentration (IC_{50}) of Rec^+ and Rec^- ($R_{50} = IC_{50,Rec+}/IC_{50,Rec-}$) [36,37].

4. Results and discussion

4.1. HBCD biodegradation by R. palustris

The activated *R. palustris* (YSC3) and the sterilized cell culture (SYSC3) in PNSB medium were subjected to HBCD treatment with a concentration of 1 mg/L. Sole 1 mg/L HBCD in the PNSB medium was considered as a positive control. The residual HBCD concentration was determined at hours 0, 4, 12, 24, 48, and 72. HBCD was removed by 20 % at 24 hr, and in a total 60 % of HBCD was degraded after 72 h (Fig. S2). However, around 20 % of HBCD removal was also observed in SYSC3, suggesting that the absorbance effect by *R. palustris*. Therefore, the actual degradation percentage of HBCD by viable *R. palustris* was approximately 40 % after 48 hr of incubation.

The metabolically diverse and well-characterized features of *R. palustris* had been proved to be capable of utilizing aromatic compounds under both aerobic and anaerobic environments [38,39]. There had been reports relating to the degradation of 2-chlorophenol by chlorophenol dehalogenase and chlorophenol nicotinamide adenine dinucleotide phosphate (NADPH)-oxidoreductase (CNOR), which results in the formation of exopolysaccharide to prevent the effect of genotoxicity [40]. It was also applied to wastewater treatment to remove cyhalofop-butyl by enhanced expression of cyhalofop-butyl-hydrolyzing carboxylesterase through activation of mitogen-activated protein kinase (MAPK) signal transduction pathway [41]. In previous studies, the HBCD removal and bromide ion release by *R. palustris* intracellular enzyme in carbon source depleted L2 medium with the degradation kinetics of 0.17 ± 0.0048 (day^{-1}) was observed [19,20,42]. The detection of HBCD metabolites, PBCDE, PBCDOH, and TBCDOH after 2 days of incubation indicated the potential contributions of debromination and hydroxylation pathways in the biotransformation of HBCD in *R. palustris* [19,20].

Previously, Wang et al. [20] have hypothesized the HBCD degradation was likely through the debromination pathway, which was catalyzed by the dehalogenases, followed by hydroxylation to cleave the ring structure. Then glutathione S-transferases (GSTs) and haloacid dehalogenases (HADHs) further completed the HBCD debromination process, and the residues were metabolized possibly through the glyoxylate cycle [20]. However, what specific functional genes and enzymes could contribute to the HBCD metabolism were yet unclear. HBCD was known to have cytotoxic effects on *Escherichia coli* and human hepatoma HepG2 cell on multiple levels, including amino acid metabolisms, DNA damage repair, and fatty acid metabolism. [43,44]. The *B. subtills* Rec assay presented an adverse effect on the survival rate when the HBCD concentration exceeded one μM (Fig. S3b). However, Chang et al.[19] showed that *R. palustris* YSC3 could maintain growth after being treated with 1 ppm HBCD, suggesting minimal toxicity. Furthermore, the HBCD metabolites after 10 days of treatment also showed no genotoxicity effect (Fig. S3c). With this, we hypothesized that *R. palustris* YSC3 modulated its regulatory response to detoxify HBCD and utilized it as biomass in the process.

4.2. RNA-seq assembly and co-expression network analysis

In order to investigate the molecular mechanism of the *R. palustris* response to HBCD treatment, the *R. palustris* transcriptional profiles in variate conditions by Illumina sequencing platform were performed. Raw data was average 1.92E + 07 reads. Quality control of raw data was conduct by Trim Galore (Table S1). Clean reads were average of 1.92E + 07 reads. Reads with quality control were mapped to *R. palustris* strain YSC3 assembled genome by HISAT2 and assembled to transcripts by StringTie. The results showed 4961 transcripts and 4907 genes were mapped against the reference genome [18]. Gene expression profiles were normalized to FPKM value and import into MOLAS system, the web-based analysis platform, for further analysis. In oder to remove low-quality transcripts, transcripts with FPKM values lower or equal to 0.001 were regarded as the noise signal, and their FPKM value would set to 0.

To analyze the gene expression in the response of *R. palustris* to HBCD treatment, we used WGCNA to examine the highly correlated gene clusters. Genes with high topological correlation were grouped into the modules. The network was built according to the transcriptional profiles at 25 °C and 35 °C, separately (Fig. 1a). Furthermore, the up-regulated gene transcripts increased in response to HBCD treatment over time were examined. The "HBCD_Time" definition was set to represent this trait and made correlations with gene modules (Fig. S5). The blue module in the 35 °C networks and the turquoise module in the 25 °C networks were the highest correlated with "HBCD_Time." As *R. palustris* YSC3 had higher HBCD removal efficiency at 35 °C, we analyzed the

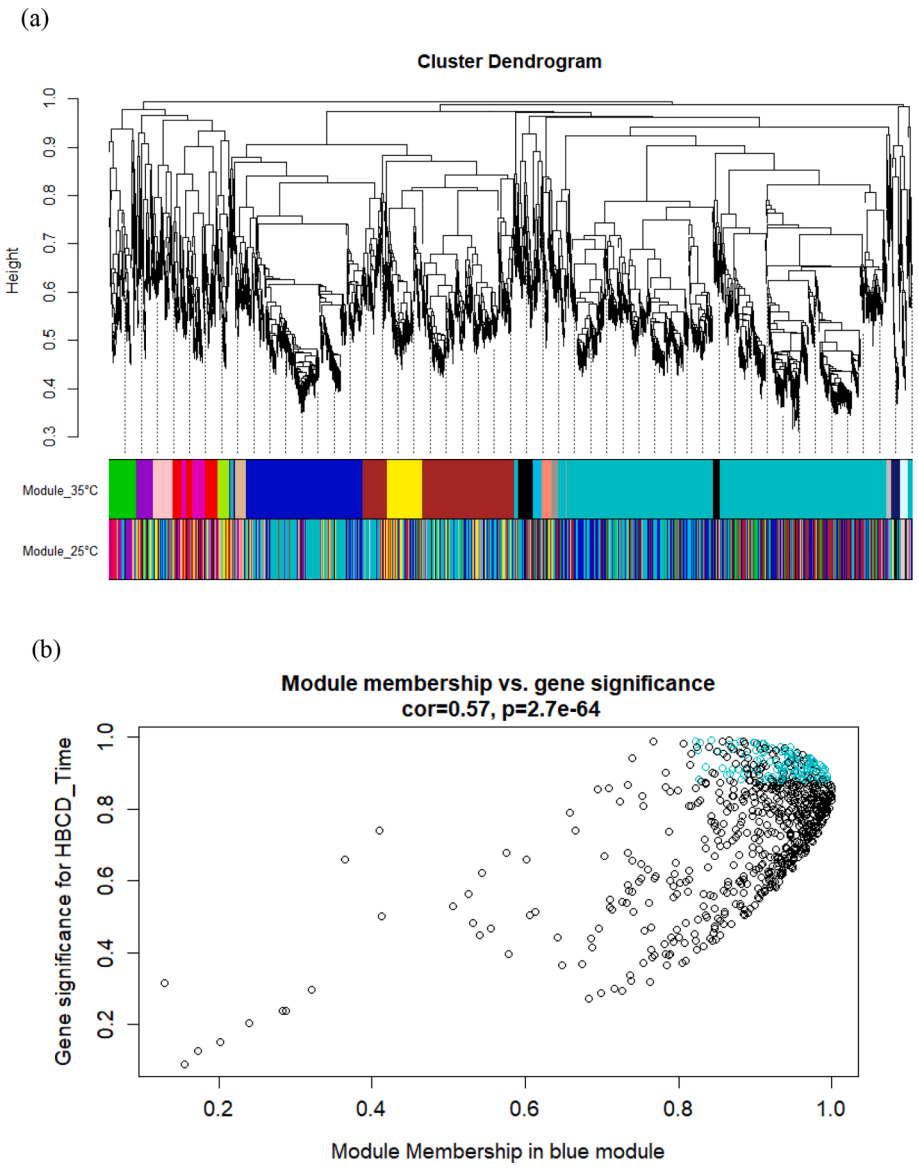

Fig. 1. Co-expression network analysis on *R. palustris* transcriptome. (a) The cluster dendrogram plot for 4961 transcripts. The dendrogram was derived from transcriptomic expression at 35 °C. There were 18 modules in the 35 °C network and 15 modules in the 25 °C network, each module with a different color. (b) The blue module's scatter plot represents the gene significance for "HBCD_Time" versus the module membership in the blue module. The genes overlapped with the turquoise module in the 25 °C networks are marked with turquoise color. (c) The heatmap plot of overlapping transcripts. Each column and row represents sample and transcript expression, respectively.

intramodular performance of the blue module in the 35 °C networks (Fig. 1b). The results showed that transcripts in the blue module also showed a high correlation (cor = 0.57, P = 2.7e-64) between GS and MM. We further inspected the overlap between blue and turquoise modules and found 126 overlapping transcripts marked with turquoise color in Fig. 1b. We build the heatmap to examine the transcript expression (Fig. 1c). The HBCD treatment group contained the most significant number of highly expressed genes, such as ferredoxin, ABC transporter, cytochrome P450, et cetera. According to the hierarchical results, the control and HBCD treated groups were separately clustered. Besides, 99 transcripts expressed higher at 35 °C and 27 transcripts at 25 °C.

The genes in the blue module which expression highly affected by HBCD were selected for GO and KEGG pathway analysis to explore their biological functions further. A total of 10 GO terms and 10 pathways ($p < 0.05$) were identified, as shown in Fig. 2. The most significantly enriched GO terms for HBCD treatment were DNA integration, single-organism carbohydrate metabolic process, and dephosphorylation, as shown in Fig. 2a. Similarly, the significant pathways for HBCD-related mRNAs were mainly enriched in the ABC transporter, butanoate metabolism, arginine/lysine biosynthesis, and bacterial secretion system, as shown in Fig. 2b.

4.3. Differential expression genes analysis

Differential expression genes (DEGs) in every four HBCD-treated groups were composed of genes up-regulated ($\log_2$ FPKM$\geq$2) and down-regulated ($\log_2$ FPKM$\leq$2) according to their FPKM values. As Fig. S4 shows, more genes were up-regulated upon the presence of HBCD treatment. On average, the number of up-regulated genes was 5-times more than the number of down-regulated genes in every HBCD-treated group, which exemplified that HBCD under the experimental condition

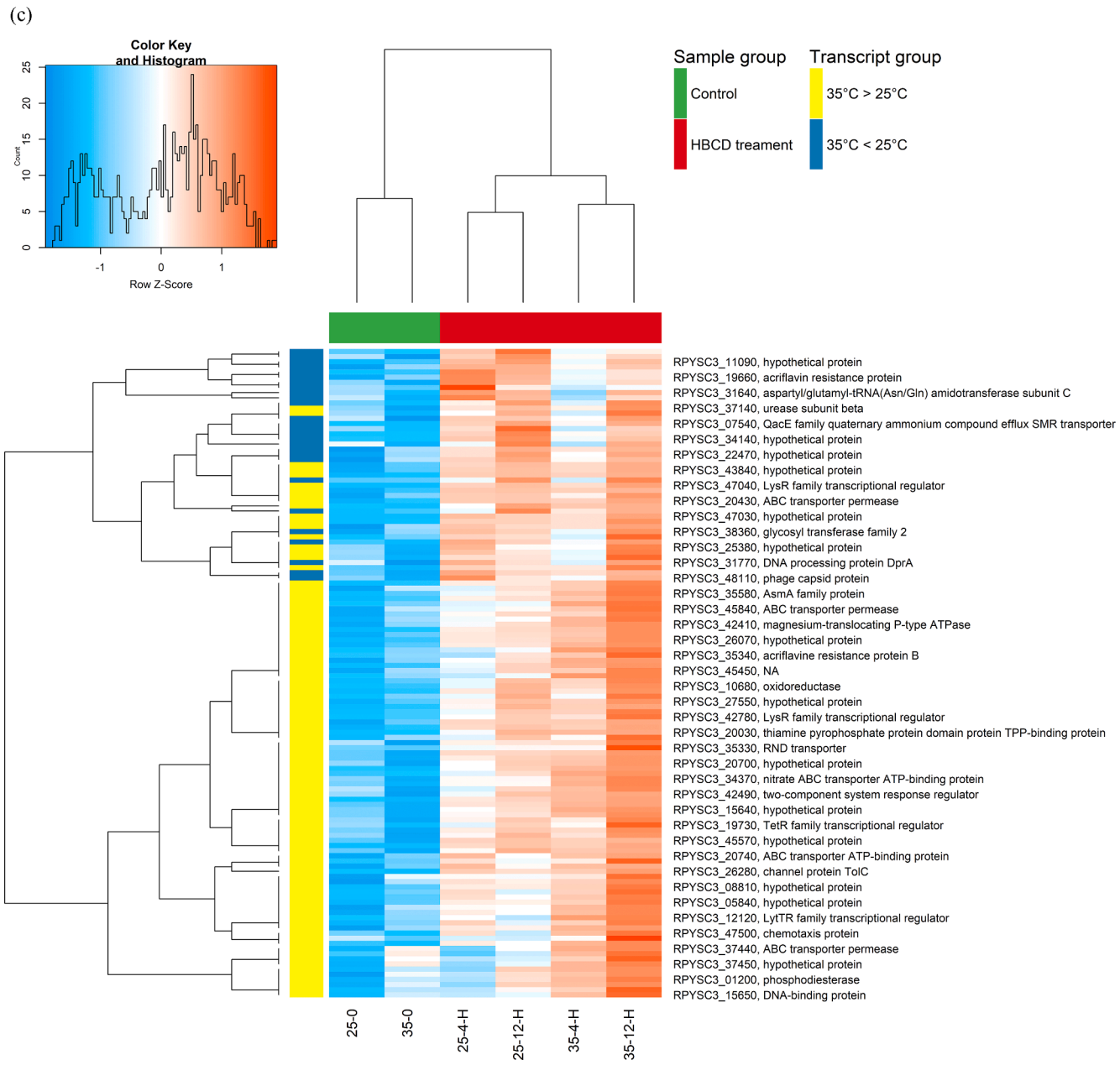

Fig. 1. (*continued*).

activated specific metabolic processes of HBCD-treated cells. To further study the characteristics of gene expression profiles of the HBCD-treated cells, several genes were randomly selected from the DEGs list of the 12 h-HBCD treatment group at 35 °C (Fig. 3a and Table S2) and were imported for PCA procedure. The PCA of the gene expression data separated HBCD-treated groups from the rest of the two control groups, which were circulated by the green dashed lines, namely 25–0 and 35–0 (Fig. 3b). The PCA data also showed a separation within the four HBCD-treated samples, namely 25–4-H, 25–12-H, 35–4-H, and 35–12-H. Although the four HBCD-treated samples were clustered near each other, the 25–4-H sample formed a relatively isolated group that separated itself from the other HBCD treated samples, suggesting the gene expression profile of the 25–4-H sample was unlike those of other HBCD treated samples. The 35–4-H and 35–12-H samples regulated relatively similar gene sets in cells containing those of the genes responsible for the degradation of aromatic compounds (indicated by Tiffaney Blue) and ABC transporters (indicated by Prussian Blue) according to the gene list (Table S2). In other words, the patterns of genes regulated by the two control groups (25–0 and 35–0) differed from that of the HBCD treated groups (35–4-H and 35–12-H) to a greater extent than the non-HBCD treated groups (25–4, 25–12, 35–4, and 35–12) (Fig. 3c), and notably with p450, GST, two-component system response regulator (TCS), cytochrome *c* (CYTC), lysR family transcriptional regulator (LYSR), ferredoxin (FER), and possible protocatechuate 4,5-dioxygenase small subunit (PC-DiOXY) showing the most distinctly different pattern of gene regulation.

To further illustrate the gene expression differences among all samples, without using the temperature as the grouping factor, 35 DEGs with high- FPKM values in the 35 °C treatment group were selected out for PCA analysis, two genes within these selected DEGs have the opposite expression profiles. Heatmap plot and hierarchical clustering were also performed. According to the heatmap results (Fig. 4), three groups separated based on their gene expression. For example, the control groups had more expression in oxidoreductase. The control groups showed relatively higher expression in succinyl-CoA ligase, malate dehydrogenase, et cetera. The HBCD treatment group contained the most

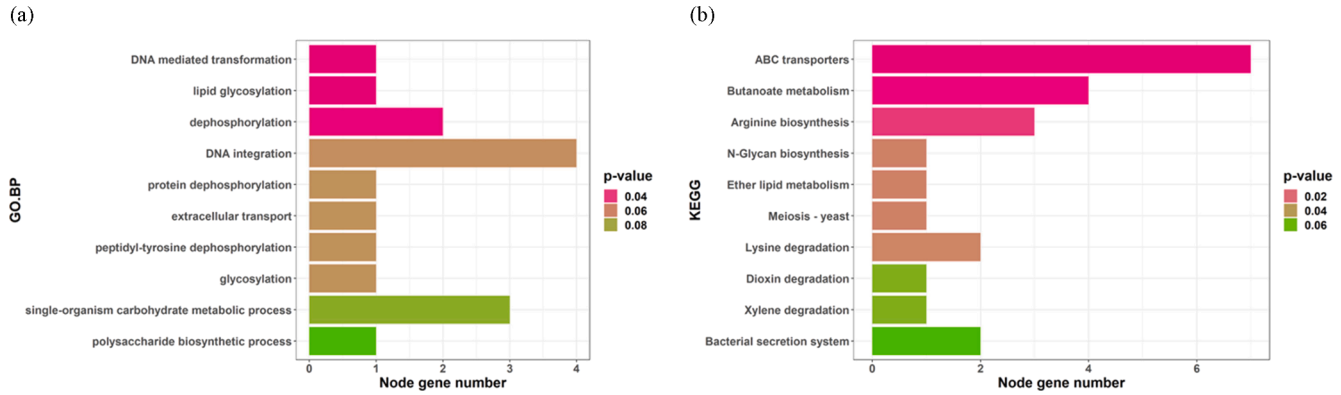

Fig. 2. GO (a) and KEGG (b) pathway enrichment analysis for HBCD-related mRNAs. Y-axis represents the enriched GO terms; X-axis (a) represents the amount of the HBCD-related mRNAs enriched in GO terms; X-axis (b) represents the amount of the HBCD-related mRNAs enriched in KEGG terms. GO, Gene Ontology; KEGG, Kyoto Encyclopedia of Genes and Genomes.

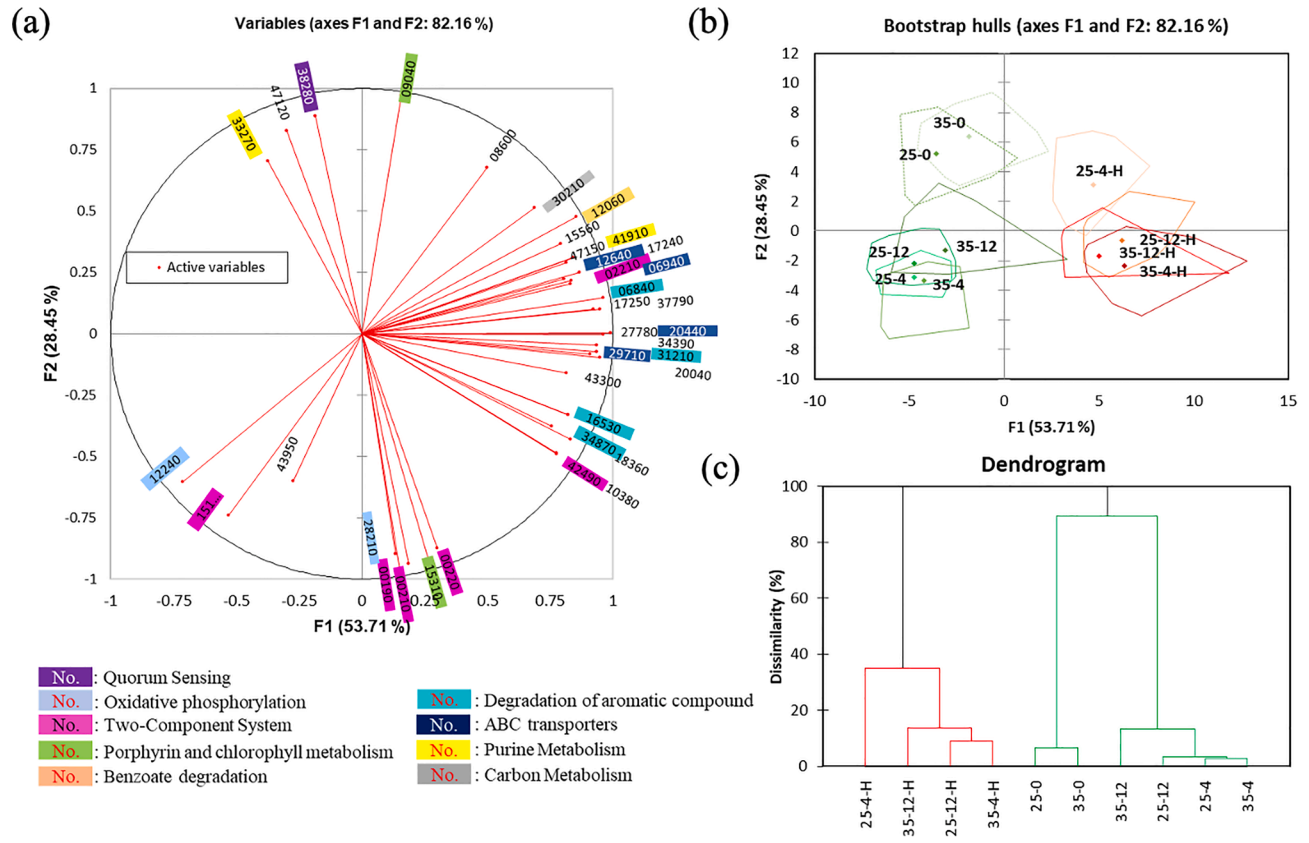

Fig. 3. Principal component analysis of differentially expressed genes (DEGs) reveals HBCD-specific segregation of different groups. (a) PCA-Correlation loadings plot of the variables (mRNA gene expression) in the principal components PC1 and PC2. Arrows indicate genes that drive the differences between groups of (b). Arrowheads pointed to a particular group indicate genes expressed at a greater relative abundance level in those samples with different treatments.

significant number of highly expressed genes, such as ferredoxin, ABC transporter, cytochrome P450, et cetera. Besides, after external stimulation, cytochrome cbb3 oxidase expression increased in both the control and HBCD treatment groups.

4.4. *Differential expressed genes of R. Palustris for HBCD biotransformation*

Besides the transcriptomics analysis for the response of *R. palustris* to HBCD exposure, and the PCA analysis for the correlation of FPKM value with HBCD treatment and temperature condition, the mRNA gene expression level was also observed through qRT-PCR approach to verify the results of RNA-seq. Based on the results of PCA analysis, we selected out 12 specific gene transcripts for further qRT-PPCR analysis: cytochrome p450 (*P450*), *HADH*, *GST*, *LYSR*, *CYTC*, *TCS*, epoxide hydrolase (*EH*), *FER*, *PC-DiOXY*, 3,4-dihydroxyphenyl acetate 2,3-dioxygenase (*DHPA-OXY*), monooxygenase (*MONO-OXY*), multiplex antenna complex (*ANTE*). The overall results showed that the genes' expression level was affected more significantly in the 35 °C treatment group (Fig. 5a) then cultured at 25 °C (Fig. 5b), which corresponded to the optimal growth condition and HBCD degradation efficiency of *R. palustris* [19,20].

After HBCD treatment, the expression level of TCS increased by 2 folds under 25 °C and 4 folds under 35 °C four hours immediate after the

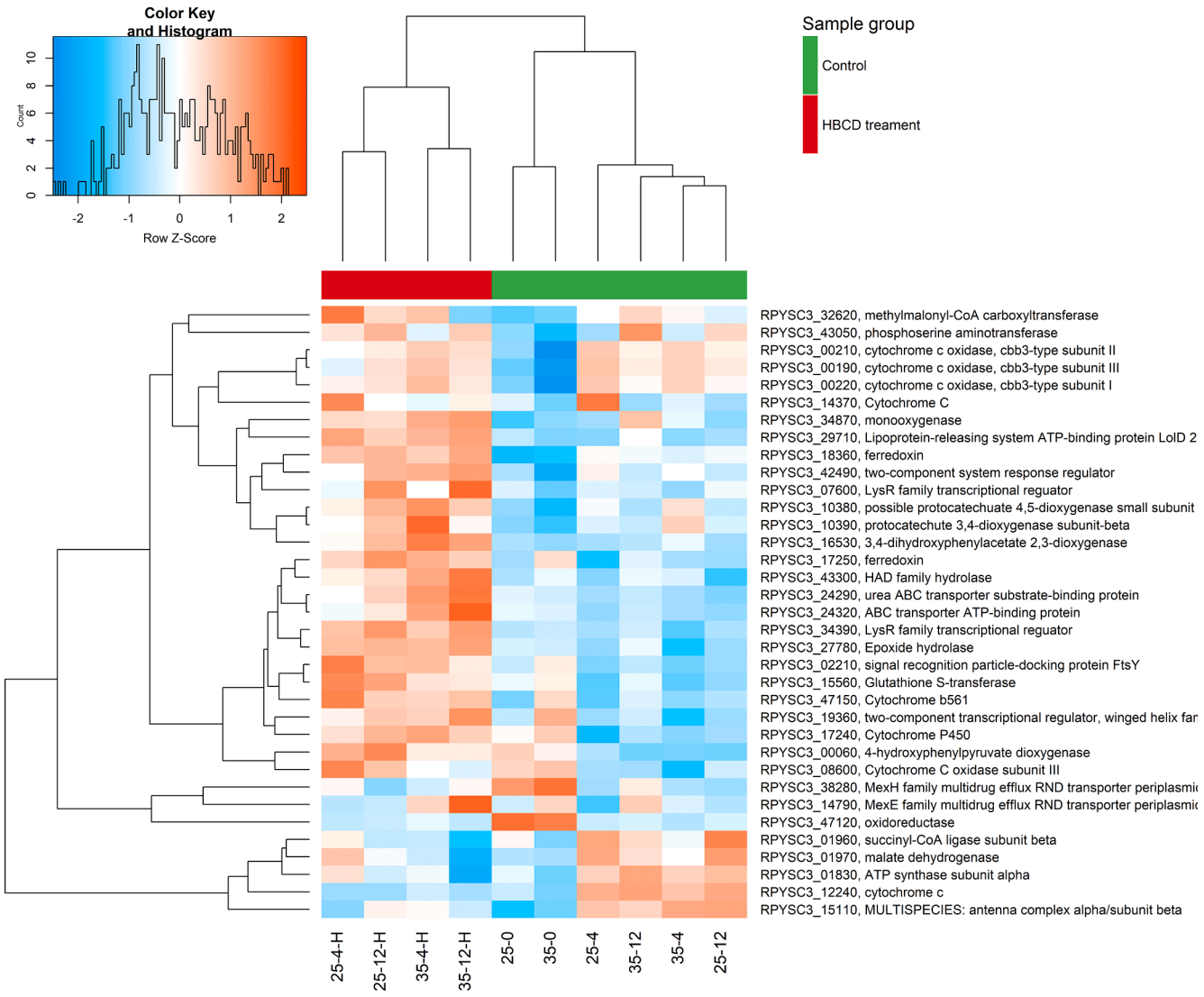

Fig. 4. Gene expression heatmap and hierarchical clustering based on DEGs between the initial, the control, and the HBCD treated groups. Each column and row represents sample and transcript expression, respectively. Each cell's color indicated a z-score of the corresponding gene. The top bar shows the type of sample. The hierarchical clustering of samples and transcript expression was based on Euclidean similarity and Spearman's rank correlation.

treatment. LysR family transcriptional factors are standard regulators to mediate the catabolic operons for organic compounds degradations. The expression level of LysR was suppressed under 25 °C but was significantly induced (5-fold increment) under 35 °C after incubation. These results suggested the potential involvement of TCS regulators and LysR regulators in the signal transduction and metabolic pathways regulations for HBCD biotransformation.

Plenty have described the regulation of xenobiotics degradation [45]. Typical TCSs comprised of a sensor histidine kinase (SHK) with a periplasmic sensing and an intracellular phosphokinase domain, and a response regulator (RR) that included a signal receiver and an output domain [46,47]. TCSs could respond to various kinds of environmental signals, e.g., pH, temperature, osmotic stress, xenobiotics, antibiotics, and triggered downstream regulations. For instance, the dioxygenase-mediated toluene degradation pathway in *Pseudomonas putida* F1 was under the regulation of the t*odXFC1C2BADEGIH* operon, which was controlled by TodS-TodT two-component regulatory system [46,48]. LysR-type transcriptional regulators (LTTRs) composed one of the most abundant identified regulatory proteins. Many of which have been proved to be associated with the degradation of hydrocarbons or aromatic pollutants [45,49]. LysR family transcriptional factors, such as CatR, ClcR and LinR, were mainly linked to the detection of aromatic organohalides (e.g. chlorophenol, chlorobenzoate) [49].

Under 35 °C, *Cyt C* and *p450* expressed increased by 3-fold and 5-fold, respectively, 12 hrs after treatment; while the expression level of *HADH* and *GST* raised by around 2-fold (Fig. 5b). However, these functional genes with dehalogenation and oxidation capacities were not considerably induced under 25 °C, which may explain the relatively low degradation rate of *R. palustris* under 25 °C (Fig. 5a) [19,20]. Studies have shown many applications of *GST*, *Cyt C*, *p450*, and *HADH* on organohalides bioremediations. Fluoroacetate dehalogenase (FAcD) of *R. palustris* (RPA1163), a member of HADH family, was reported to break the C-F bond, which was considered the strongest C-halogen bond, by a S_N2 reaction, and degrade polyfluorocarboxylic acids [50,51]. The GST31 and CYP71C3v2 in maize were described to have enantiomer's preference for HBCDs and degrade HBCD through debromination and hydroxylation metabolisms [52]. Ring cleavage enzymes are essential for microbial degradation of xenobiotics to convert to aliphatic compounds, which could be more accessible for downstream metabolisms [53]. Protocatechuate dioxygenases have long been recognized as crucial enzymes for ring cleavages and were widely discovered in soil-borne fungus or bacterium or marine bacterial ecology [54,55]. Our study with *R. palustris* also revealed a higher expression level of protocatechuate 4,5-dioxygenase (Fig. 5) 4 hrs after HBCD treatment

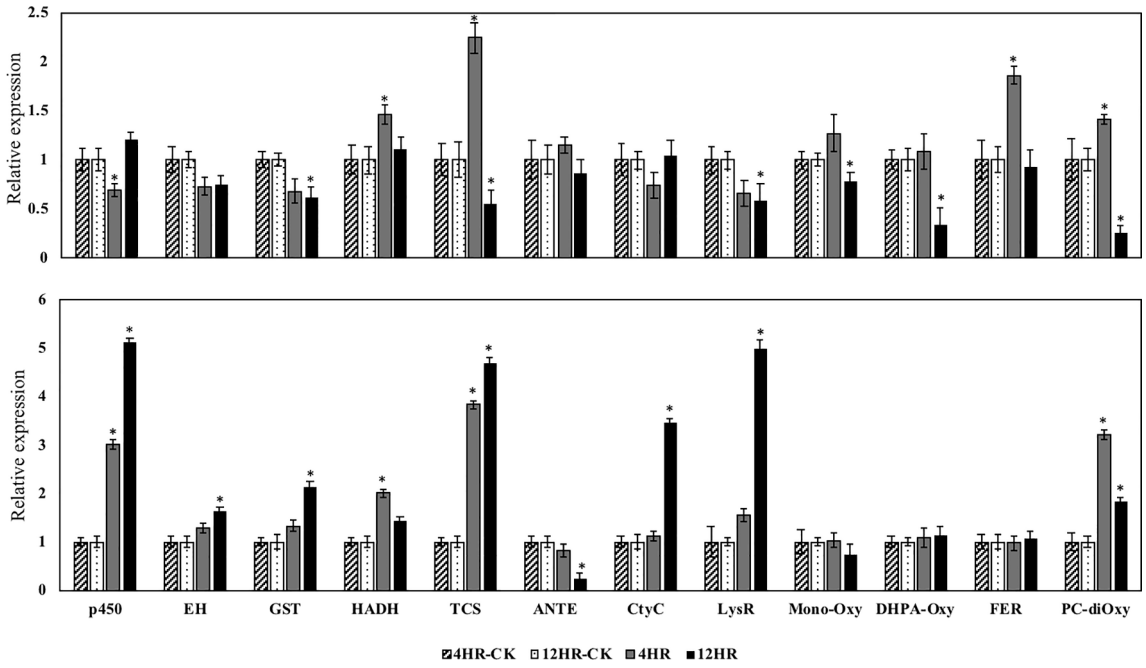

Fig. 5. HBCD biotransformation-related gene relative expression in *R. palustris*. (a) The genes expression level of *R. palustris* at 25 °C. (b) The gene expression level of *R. palustris* at 35 °C. The asterisks indicate significant differences between the treatment group and CK, p-value < 0.05.

indicated the ring cleavage metabolisms for HBCD degradation. Overall, the gene expression level of enzymes with HBCD degrading functions were elevated.

4.5. Presumed HBCD biotransformation pathway in R. palustris

Studies have delineated similar aromatic xenobiotic degradation pathways in certain microbes. In the beginning, microbial photosynthesis genes modulated according to light quality were generally considered to be involved in the degradation of aromatic compounds commonly found in agricultural wastes [16]. Similarly, a more recent study of the microbial HBCD degradation shown related genes annotated to the photosynthesis system in the GO term and involved in the redox signaling in KEGG pathways, including regulatory *RegA* (RP05970) genes, *CcoN* (RP00220), *CcoO* (RP010210), *CcoP* (RP00190), and *CcoQ* (RP00200) [20]. These cytochrome cbb3 oxidase-related proteins mentioned above are present in *R. pslustris* in this study and were responsible for the degradation of 2,4,6-trinitrotoluene in *Pseudomonas putida* [56]. Besides, enzymes such as dioxygenase, peroxidase, P450 monooxygenase, and dehalogenase were previously shown for the degradation of polychlorinated dibenzo-p-dioxins and polychlorinated dibenzofurans [57-59], had their roles in HBCD degradation in this

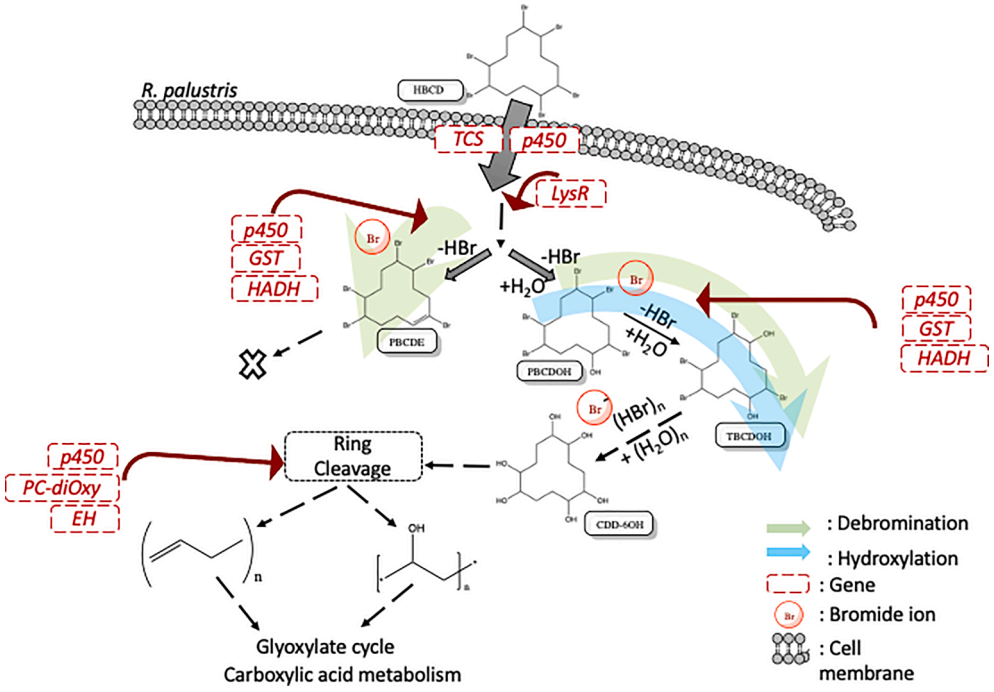

Fig. 6. Presumed signal pathway of HBCD degradation in *R. palustris* based on transcriptomic approach. The green arrow represents the debromination metabolic pathway; the blue arrow stands for the hydroxylation process. TCS: two-component system regulator, p450: cytochrome p450, LysR: LysR transcriptional regulator, GST: glutathione S-transferase, HADH: haloacid dehalogenase protein family. PC-diOxy: Protocatechuate 4,5-dioxygenase. EH: Epoxide hydrolase. One novel strain, *Rhodopseudomonas palustris* YSC3, can degrade HBCD.

study (Fig. 6). The carbon atom derived from the degradation of HBCD could be used as a type of carbon source by *Achromobacter* sp. for growth [60]. Wang et al. [20] proposed that the degradation of HBCD in *R. pslustris* was first through the partial debromination reactions via debromination enzymes with stereo-selectivity. These were followed by an open-ring reaction before the completion of the debromination process [20]. During the degradation, 2-bromo acetyl aldehyde and then 2-bromoacetate were formed and sequentially dibrominated to form glycolic acid, which enters the glyoxylate cycle as a carbon source for cell growth [20].

In this study, more genes involved in the degradation of HBCD were identified. Accompany with the genes previously mentioned *R. palustris* during HBCD degradation, we were able to propose a more comprehensive HBCD degradation pathway. Together with the results shown in Fig. 6, we propose that during the degradation of HBCD, whether it is in the degraded or original form of HBCD, it will first act as a ligand that binds to the receptors of the TCS situated on the outer cell membrane, a transmembrane protein with their ligand-binding domain on the outer surface of the plasma membrane. This binding activates those signaling pathways that immediately transfer the phosphate to a second intracellular signaling protein [61]. Although this activation process coincides with HBCD treatment, a genetic feedback control system induces HBCD degradation pathways when TCS expression is downregulated (this can be seen in the 25–12-H group). The up-regulated *p450* (RPYSC3_17240) gene in the 35–4-H and 35–12-H is the class II cytochromes P450, which is one of the two-component systems made up of a FAD-containing, flavin mononucleotide (FMN)-containing NADPH-dependent cytochrome P450 reductase [62]. Therefore, it is involved in the sensing of environmental stimulus and responsible for the degradation of HBCD (Fig. 6). Indeed, the expression of GST increased under the control of LysR-Type transcriptional regulators and this relationship could be seen in another study, which uses *Pseudomonas aeruginosa* as their studying material [63]. Interestingly, our results provide further evidence that HAHD was possibly as well controlled by LysR-Type transcriptional regulators that previously proposed in the haloacid dehalogenase repressor (hdhR) knockout mutant of *Sinorhizobium meliloti* [64]. What is equally crucial about this paper is that although some of the gene clusters were discussed in the HBCD degradation pathways, genes that were down-regulated and had not been thoroughly investigated still paved the way for future studies.

5. Conclusion

Time-course transcriptome analysis revealed that the cellular mechanism by which HBCD degradation observed in this study, involves unique expression characteristics (Fig. 5), i.e., both hydroxylation and debromination pathways were used for HBCD degradation. This was different from other microbial modes of HBCD degradation, i.e., aerobic hydroxylation and anaerobic debromination, which demonstrate that there are fewer restrictions on oxygen demand for both reactions to occur. The strategies while integrating the time and temperature as variables let us know more about the functions of gene clusters (or modules mentioned in this study) that work together to tackle similar biochemical tasks in terms of HBCD degradation. Expressly, the regulators for HBCD degradation enzymes were confirmed, which include transmembrane proteins of class II cytochromes P450 and the TCS; higher levels of gene expression precisely controlled by the LysR-Type transcriptional regulators including GST and HAHD during more extended HBCD treatment condition reveals the appropriate transitioning of HBCD tolerance state to positive degradation. The gene expression trends derived from the transcriptomic analysis showed good correlations with the qPCR results. Although transcriptional regulation is essential for studying new pathways, a clearer understanding of the enzyme-substrate binding mechanism and specificity requires additional efforts, including gene cloning, mutant cells, and byproduct analyses. However, combining the transcriptomic profiles data and gene expression level analysis, this work strongly demonstrates an in-depth research way into the molecular basis to study the microbial biotransformation mechanism and provides a web-based analysis platform, MOLAS for researchers. The approaches introduced in this study were relatively new in this field, which would become a template for future studies for better understanding onmicrobial degradation of difficult chemicals like BFRs or POPs in the environment.

Declaration of Competing Interest

The authors declare that they have no known competing financial interests or personal relationships that could have appeared to influence the work reported in this paper.

Acknowledgments

Research grants from Taiwan's Ministry of Science and Technology (No. 106-2221-E-002 -043 -MY3) and the joint program of National Taiwan University and Academia Sinica, Taiwan (NTU-AS-109L104312 and NTU-AS-110L104312) support this work. We also thank the High Throughput Sequencing Core hosted in the Biodiversity Research Center at Academia Sinica for performing the NGS experiments.

Appendix A. Supplementary data

Supplementary data to this article can be found online at https://doi.org/10.1016/j.cej.2021.130489.

References

[1] G. Yu, Q. Bu, Z. Cao, X. Du, J. Xia, M. Wu, J. Huang, Brominated flame retardants (BFRs): A review on environmental contamination in China, Chemosphere 150 (2016) 479–490.
[2] C.H. Marvin, G.T. Tomy, J.M. Armitage, J.A. Arnot, L. McCarty, A. Covaci, V. Palace, Hexabromocyclododecane: Current understanding of chemistry, environmental fate and toxicology and implications for global management, Environ. Sci. Technol. 45 (2011) 8613–8623.
[3] L. Huang, S.B. Shah, H. Hu, P. Xu, H. Tang, Pollution and biodegradation of hexabromocyclododecanes: A review, Frontiers of Environmental Science & Engineering 14 (2019) 11.
[4] C. Koch, T. Schmidt-Kötters, R. Rupp, B. Sures, Review of hexabromocyclododecane (HBCD) with a focus on legislation and recent publications concerning toxicokinetics and dynamics, Environ. Pollut. 199 (2015) 26–34.
[5] J. Hiebl, W. Vetter, Detection of hexabromocyclododecane and its metabolite pentabromocyclododecene in chicken egg and fish from the official food control, J. Agric. Food. Chem. 55 (9) (2007) 3319–3324.
[6] B.P. L. Webster, J. Tronczynski, K. Vorkamp, P. Lepom, Determination of hexabromocyclododecane (HBCD) in sediment and biota, ICES Techniques in Marine, Environmental Sciences (2010) 15.
[7] A. Schecter, D.T. Szabo, J. Miller, T.L. Gent, N. Malik-Bass, M. Petersen, O. Paepke, J.A. Colacino, L.S. Hynan, T.R. Harris, S. Malla, L.S. Birnbaum, Hexabromocyclododecane (HBCD) stereoisomers in U.S. food from Dallas, Texas, Environ Health Perspect 120 (9) (2012) 1260–1264.
[8] H. Hakk, D.T. Szabo, J. Huwe, J. Diliberto, L.S. Birnbaum, Novel and distinct metabolites identified following a single oral dose of α- or γ-Hexabromocyclododecane in mice, Environ. Sci. Technol. 46 (24) (2012) 13494–13503.
[9] Q. Li, L. Wang, X. Fang, L. Zhang, J. Li, H. Xie, Synergistic effect of photocatalytic degradation of hexabromocyclododecane in water by UV/TiO_2/persulfate, Catalysts 9 (2019) 189–202.
[10] C.-ping. Tso, Y.-hsin. Shih, The transformation of hexabromocyclododecane using zerovalent iron nanoparticle aggregates, J. Hazard. Mater. 277 (2014) 76–83.
[11] S.L. Waaijers, J.R. Parsons, Biodegradation of brominated and organophosphorus flame retardants, Curr. Opin. Biotechnol. 38 (2016) 14–23.
[12] M. Megharaj, B. Ramakrishnan, K. Venkateswarlu, N. Sethunathan, R. Naidu, Bioremediation approaches for organic pollutants: A critical perspective, Environ. Int. 37 (2011) 1362–1375.
[13] T. Yamada, Y. Takahama, Y. Yamada, Isolation of *Pseudomonas* sp. Strain HB01 which degrades the persistent brominated flame retardant γ-Hexabromocyclododecane, Biosci. Biotechnol. Biochem. 73 (2009) 1674–1678.
[14] L. Huang, W. Wang, S.B. Shah, H. Hu, P. Xu, H. Tang, The HBCDs biodegradation using a *Pseudomonas* strain and its application in soil phytoremediation, J. Hazard. Mater. 380 (2019), 120833.
[15] X. Shen, H. Hu, H. Peng, W. Wang, X. Zhang, Comparative genomic analysis of four representative plant growth-promoting rhizobacteria in *Pseudomonas*, BMC Genomics 14 (2013) 271.

[16] F.W. Larimer, P. Chain, L. Hauser, J. Lamerdin, S. Malfatti, L. Do, M.L. Land, D. A. Pelletier, J.T. Beatty, A.S. Lang, F.R. Tabita, J.L. Gibson, T.E. Hanson, C. Bobst, J.L.T.y. Torres, C. Peres, F.H. Harrison, J. Gibson, C.S. Harwood, Complete genome sequence of the metabolically versatile photosynthetic bacterium *Rhodopseudomonas palustris*, Nat. Biotechnol. 22 (1) (2004) 55–61.

[17] A. Adessi, R. De Philippis, Purple Bacteria: Electron Acceptors and Donors, in: W. J. Lennarz, M.D. Lane (Eds.), Encyclopedia of Biological Chemistry (Second Edition), Academic Press, Waltham, 2013, pp. 693–699.

[18] K.J. Lo, S.S. Lin, C.W. Lu, C.H. Kuo, C.T. Liu, Whole-genome sequencing and comparative analysis of two plant-associated strains of *Rhodopseudomonas palustris* (PS3 and YSC3), Sci. Rep. 8 (2018) 12769.

[19] T.H. Chang, R. Wang, Y.H. Peng, T.H. Chou, Y.J. Li, Y.h. Shih, Biodegradation of hexabromocyclododecane by *Rhodopseudomonas palustris* YSC3 strain: A free-living nitrogen-fixing bacterium isolated in Taiwan, Chemosphere 246 (2020), 125621.

[20] R. Wang, C.Y. Lin, S.H. Chen, K.J. Lo, C.T. Liu, T.H. Chou, Y.h. Shih, Using high-throughput transcriptome sequencing to investigate the biotransformation mechanism of hexabromocyclododecane with *Rhodopseudomonas palustris* in water, Sci. Total Environ. 692 (2019) 249–258.

[21] D.H. Pieper, Vítor.AP. Martins dos Santos, P.N. Golyshin, Genomic and mechanistic insights into the biodegradation of organic pollutants, Curr Opin Biotechnol 15 (3) (2004) 215–224.

[22] Y.-H. Peng, Y.-jou. Chen, M. Chang, Y.-hsin. Shih, Shih, The effect of zerovalent iron on the microbial degradation of hexabromocyclododecane, Chemosphere 200 (2018) 419–426.

[23] Y. Moriya, M. Itoh, S. Okuda, A.C. Yoshizawa, M. Kanehisa, KAAS: an automatic genome annotation and pathway reconstruction server, Nucleic Acids Res 35 (Web Server) (2007) W182–W185.

[24] E. Afgan, D. Baker, B. Batut, M. van den Beek, D. Bouvier, M. Cech, J. Chilton, D. Clements, N. Coraor, B.A. Grüning, A. Guerler, J. Hillman-Jackson, S. Hiltemann, V. Jalili, H. Rasche, N. Soranzo, J. Goecks, J. Taylor, A. Nekrutenko, D. Blankenberg, The Galaxy platform for accessible, reproducible and collaborative biomedical analyses, Nucleic Acids Res. 46 (2018) (2018) W537–W544.

[25] M. Martin, Cutadapt removes adapter sequences from high-throughput sequencing reads 2011 (17) (2011) 3.

[26] D. Kim, B. Langmead, S.L. Salzberg, HISAT: a fast spliced aligner with low memory requirements, Nat. Methods 12 (2015) 357–360.

[27] M. Pertea, G.M. Pertea, C.M. Antonescu, T.-C. Chang, J.T. Mendell, S.L. Salzberg, StringTie enables improved reconstruction of a transcriptome from RNA-seq reads, Nat. Biotechnol. 33 (3) (2015) 290–295.

[28] C. Trapnell, A. Roberts, L. Goff, G. Pertea, D. Kim, D.R. Kelley, H. Pimentel, S. L. Salzberg, J.L. Rinn, L. Pachter, Differential gene and transcript expression analysis of RNA-seq experiments with TopHat and Cufflinks, Nat Protoc 7 (3) (2012) 562–578.

[29] P. Langfelder, S. Horvath, Fast R functions for robust correlations and hierarchical clustering, J Stat Softw 46 (11) (2012), https://doi.org/10.18637/jss.v046.i11.

[30] P. Langfelder, S. Horvath, WGCNA: an R package for weighted correlation network analysis, BMC Bioinf. 9 (2008) 559.

[31] Z. Gu, R. Eils, M. Schlesner, Complex heatmaps reveal patterns and correlations in multidimensional genomic data, Bioinformatics (Oxford, England) 32 (2016) 2847–2849.

[32] S.A. Bustin, V. Benes, J.A. Garson, J. Hellemans, J. Huggett, M. Kubista, R. Mueller, T. Nolan, M.W. Pfaffl, G.L. Shipley, J. Vandesompele, C.T. Wittwer, The MIQE guidelines: minimum information for publication of quantitative real-time PCR experiments, Clin Chem 55 (2009) 611–622.

[33] J. Ye, G. Coulouris, I. Zaretskaya, I. Cutcutache, S. Rozen, T.L. Madden, Primer-BLAST: A tool to design target-specific primers for polymerase chain reaction, BMC Bioinf. 13 (2012) 134.

[34] P. Ma, T. Mori, C. Zhao, T. Thiel, C.H. Johnson, Evolution of KaiC-Dependent timekeepers: A proto-circadian timing mechanism confers adaptive fitness in the purple bacterium *Rhodopseudomonas palustris*, PLoS Genet. 12 (2016), e1005922.

[35] R. Singh, T.O. Ranaivoarisoa, D. Gupta, W. Bai, A. Bose, I. Cann, Genetic redundancy in iron and manganese transport in the metabolically versatile bacterium *Rhodopseudomonas palustris* TIE-1, Appl. Environ. Microbiol. 86 (16) (2020), https://doi.org/10.1128/AEM.01057-20.

[36] P.H. Chou, C.H. Chen, K.Y. Chen, F.C. Ko, T.Y. Tsai, Y.P. Yeh, Assessing the endocrine disrupting potentials and genotoxicity in environmental samples from Taiwanese rivers, Genes Environ. 41 (2019) 24.

[37] H. Takigami, S. Matsui, T. Matsuda, Y. Shimizu, The *Bacillus subtilis* rec-assay: a powerful tool for the detection of genotoxic substances in the water environment, Prospect for assessing potential impact of pollutants from stabilized wastes, Waste Management 22 (2002) 209–213.

[38] C.S. Harwood, J. Gibson, Anaerobic and aerobic metabolism of diverse aromatic compounds by the photosynthetic bacterium *Rhodopseudomonas palustris*, Appl. Environ. Microbiol. 54 (1988) 712.

[39] T.V. Karpinets, D.A. Pelletier, C. Pan, E.C. Uberbacher, G.V. Melnichenko, R. L. Hettich, N.F. Samatova, M. Isalan, Phenotype Fingerprinting Suggests the Involvement of Single-Genotype Consortia in Degradation of Aromatic Compounds by *Rhodopseudomonas palustris*, PLoS ONE 4 (2) (2009) e4615, https://doi.org/10.1371/journal.pone.000461510.1371/journal.pone.0004615.g00110.1371/journal.pone.0004615.g00210.1371/journal.pone.0004615.g00310.1371/journal.pone.0004615.g00410.1371/journal.pone.0004615.t00110.1371/journal.pone.0004615.s00110.1371/journal.pone.0004615.s00210.1371/journal.pone.0004615.s00310.1371/journal.pone.0004615.s004.

[40] K. Mutharasaiah, V. Govindareddy, K. Chandrakant, Biodegradation of 2-Chlorophenol by *Rhodopseudomonas palustris*, Biorem. J. 16 (1) (2012) 1–8.

[41] P. Wu, Z. Chen, Y. Zhang, Y. Wang, F. Zhu, B. Cao, Y. Wu, N. Li, *Rhodopseudomonas palustris* wastewater treatment: Cyhalofop-butyl removal, biochemicals production and mathematical model establishment, Bioresour. Technol. 282 (2019) 390–397.

[42] S. Suzuki, T. Aono, K.-B. Lee, T. Suzuki, C.-T. Liu, H. Miwa, S. Wakao, T. Iki, H. Oyaizu, Rhizobial factors required for stem nodule maturation and maintenance in *Sesbania rostrata-Azorhizobium caulinodans* ORS571 Symbiosis, Appl. Environ. Microbiol. 73 (2007) 6650.

[43] K. Yang, Q. Zhong, H. Qin, Y. Long, H. Ou, J. Ye, Y. Qu, Molecular response mechanism in *Escherichia coli* under hexabromocyclododecane stress, Sci. Total Environ. 708 (2020), 135199.

[44] F. Wang, H. Zhang, N. Geng, B. Zhang, X. Ren, J. Chen, New Insights into the Cytotoxic Mechanism of Hexabromocyclododecane from a Metabolomic Approach, Environ. Sci. Technol. 50 (6) (2016) 3145–3153.

[45] D. Tropel, J.R. van der Meer, Bacterial transcriptional regulators for degradation pathways of aromatic compounds, Microbiology and molecular biology reviews : MMBR 68 (3) (2004) 474–500.

[46] A. Busch, N. Mesa-Torres, T. Krell, in: Cellular Ecophysiology of Microbe, Springer International Publishing, Cham, 2018, pp. 1–21, https://doi.org/10.1007/978-3-319-20796-4_6-1.

[47] S. Tiwari, S.B. Jamal, S.S. Hassan, P.V.S.D. Carvalho, S. Almeida, D. Barh, P. Ghosh, A. Silva, T.L.P. Castro, V. Azevedo, Two-Component signal transduction systems of pathogenic bacteria as targets for antimicrobial therapy: An Overview, Front. Microbiol. 8 (2017).

[48] R.E. Parales, J.V. Parales, D.A. Pelletier, J.L. Ditty, Diversity of Microbial Toluene Degradation Pathways, Advances in Applied Microbiology, Academic Press (2008) 1–73.

[49] B. Maucourt, S. Vuilleumier, F. Bringel, Transcriptional regulation of organohalide pollutant utilisation in bacteria, FEMS Microbiol. Rev. 44 (2) (2020) 189–207.

[50] Y. Li, Y. Yue, H. Zhang, Z. Yang, H. Wang, S. Tian, J.-B. Wang, Q. Zhang, W. Wang, Harnessing fluoroacetate dehalogenase for defluorination of fluorocarboxylic acids: in silico and in vitro approach, Environ. Int. 131 (2019), 104999.

[51] S. Miranda-Rojas, I. Fernández, J. Kästner, A. Toro-Labbé, F. Mendizábal, Unraveling the nature of the catalytic power of fluoroacetate dehalogenase, ChemCatChem 10 (5) (2018) 1052–1063.

[52] H. Huang, S. Zhang, J. Lv, B. Wen, S. Wang, T. Wu, Experimental and theoretical evidence for diastereomer- and enantiomer-specific accumulation and biotransformation of HBCD in maize roots, Environ. Sci. Technol. 50 (22) (2016) 12205–12213.

[53] P. Pimviriyakul, T. Wongnate, R. Tinikul, P. Chaiyen, Microbial degradation of halogenated aromatics: molecular mechanisms and enzymatic reactions, Microb. Biotechnol. 13 (2020) 67–86.

[54] R.J.M. Lubbers, A. Dilokpimol, M. Peng, J. Visser, M.R. Mäkelä, K.S. Hildén, R. P. de Vries, Discovery of novel p-Hydroxybenzoate-m-hydroxylase, protocatechuate 3,4 ring-cleavage dioxygenase, and hydroxyquinol 1,2 ring-cleavage dioxygenase from the filamentous fungus *Aspergillus niger*, ACS Sustainable Chem. Eng. 7 (23) (2019) 19081–19089.

[55] A. Buchan, L.S. Collier, E.L. Neidle, M.A. Moran, Key Aromatic-Ring-Cleaving Enzyme, Protocatechuate 3,4-Dioxygenase, in the Ecologically Important Marine *Roseobacter* Lineage, Appl. Environ. Microbiol. 66 (2000) 4662.

[56] M. Fernández, E. Duque, P. Pizarro-Tobías, P. Van Dillewijn, R.-M. Wittich, J. L. Ramos, Microbial responses to xenobiotic compounds. Identification of genes that allow *Pseudomonas putida* KT2440 to cope with 2,4,6-trinitrotoluene, Microb, Biotechnol 2 (2) (2009) 287–294.

[57] H. Habe, J.-S. Chung, J.-H. Lee, K. Kasuga, T. Yoshida, H. Nojiri, T. Omori, Degradation of chlorinated dibenzofurans and dibenzo-p-dioxins by two types of bacteria having angular dioxygenases with different features, Appl Environ Microbiol 67 (8) (2001) 3610–3617.

[58] J. Widada, H. Nojiri, K. Kasuga, T. Yoshida, H. Habe, T. Omori, Quantification of the carbazole 1,9a-dioxygenase gene by real-time competitive PCR combined with co-extraction of internal standards, FEMS Microbiol. Lett. 202 (1) (2001) 51–57.

[59] M. Bunge, L. Adrian, A. Kraus, M. Opel, W.G. Lorenz, J.R. Andreesen, H. Görisch, U. Lechner, Reductive dehalogenation of chlorinated dioxins by an anaerobic bacterium, Nature 421 (6921) (2003) 357–360.

[60] X. Peng, X. Huang, F. Jing, Z. Zhang, D. Wei, X. Jia, Study of novel pure culture HBCD-1, effectively degrading Hexabromocyclododecane, isolated from an anaerobic reactor, Bioresour Technol 185 (2015) 218–224.

[61] F. Ahmad, D. Zhu, J. Sun, Bacterial chemotaxis: a way forward to aromatic compounds biodegradation, Environ. Sci. Eur. 32 (2020) 52.

[62] G.A. Roberts, G. Grogan, A. Greter, S.L. Flitsch, N.J. Turner, Identification of a new class of cytochrome P450 from a Rhodococcus sp, J Bacteriol 184 (14) (2002) 3898–3908.

[63] F.J. Reen, J.M. Haynes, M.J. Mooij, F. O'Gara, R.M.R. II, A non-classical LysR-type transcriptional regulator PA2206 is required for an effective oxidative stress response in Pseudomonas aeruginosa, PLoS ONE 8 (1) (2013) e54479, https://doi.org/10.1371/journal.pone.0054479.

[64] R. Sallabhan, J. Kerdwong, J.M. Dubbs, K. Somsongkul, W. Whangsuk, P. Piewtongon, S. Mongkolsuk, S. Loprasert, The hdhA gene encodes a haloacid dehalogenase that is regulated by the LysR-Type regulator HdhR, in *Sinorhizobium meliloti*, Mol. Biotechnol. 54 (2) (2013) 148–157.